Original Article

Altered effective connectivity in Parkinson's disease patients with rapid eye movement sleep behavior disorder: a resting-state functional magnetic resonance imaging study and support vector machine analysis

Ai-Di Shan[#], Heng Zhang[#], Meng-Xi Gao[#], Li-Na Wang, Xing-Yue Cao, Cai-Ting Gan, Hui-Min Sun, Qian-Ling Lu, Li Zhang, Yong-Sheng Yuan, Ke-Zhong Zhang

Department of Neurology, The First Affiliated Hospital of Nanjing Medical University, Nanjing, China

Contributions: (I) Conception and design: AD Shan, H Zhang, MX Gao; (II) Administrative support: KZ Zhang; (III) Provision of study materials or patients: YS Yuan, KZ Zhang; (IV) Collection and assembly of data: AD Shan, H Zhang, MX Gao; (V) Data analysis and interpretation: AD Shan, H Zhang; (VI) Manuscript writing: All authors; (VII) Final approval of manuscript: All authors.

[#]These authors contributed equally to this work as co-first authors.

Correspondence to: Ke-Zhong Zhang, PhD; Yong-Sheng Yuan, PhD. Department of Neurology, The First Affiliated Hospital of Nanjing Medical University, No. 300 Guangzhou Road, Nanjing 210029, China. Email: kezhong_zhang1969@126.com; da_sheng@126.com.

Background: Rapid eye movement sleep behavior disorder (RBD) is associated with pathological α-synuclein deposition and may have different damage directions due to α-synuclein spreading orientations. Recent functional imaging studies of Parkinson's disease (PD) with RBD have identified abnormalities in connectivity, but effective connectivity (EC) for this altered orientation is understudied. Here, we aimed to explore altered intrinsic functional connectivity (FC) and EC in PD patients with probable RBD (pRBD).

Methods: This was a cross-sectional study. A total of 31 PD patients with pRBD (PD-pRBD), 35 PD without pRBD (PD-npRBD), and 32 healthy controls (HCs) underwent resting-state functional magnetic resonance imaging (RS-fMRI) scans. The voxel-wise degree centrality (DC) calculation was first performed to investigate the inherent connectivity of the PD-pRBD patients. Subsequently, we applied Granger causality analysis (GCA) to probe the causal effects of anomalous brain regions. Finally, the support vector machine (SVM) method was executed to evaluate the DC values in identifying PD-pRBD.

Results: PD-pRBD patients exhibited reduced z-DC values in the right precentral gyrus relative to PD-npRBD (voxel-level $P<0.001$, cluster-level $P<0.05$), as well as decreased z-DC values in the right postcentral gyrus and the superior parietal lobule compared to HCs. Then, our GCA revealed that decreased EC was located predominantly from the right precentral gyrus to the right caudate nucleus in the PD-pRBD group. Additionally, the SVM results revealed that the z-DC values of the right precentral gyrus could discriminate PD-pRBD from the PD-npRBD group [area under the curve (AUC) =0.905].

Conclusions: The altered z-DC in the right precentral gyrus and the anomaly causal effects from the precentral motor cortex to the ipsilateral striatum represented by the caudate nucleus might play vital roles in the pathogenesis of PD-pRBD. It was speculated that the attenuation of FC from the precentral motor cortex to the subcortical striatum might be associated with nocturnal muscle dyskinesia and behavioral abnormalities in PD-pRBD patients. This disruption pattern may be a prospective imaging marker in the characterization of PD with pRBD.

Keywords: Degree centrality (DC); rapid eye movement sleep behavior disorder (RBD); Granger causality analysis (GCA); Parkinson's disease (PD); resting-state functional magnetic resonance imaging (RS-fMRI)

Submitted Jun 14, 2024. Accepted for publication Nov 06, 2024. Published online Dec 27, 2024.
doi: 10.21037/qims-24-1196
View this article at: https://dx.doi.org/10.21037/qims-24-1196

Introduction

Rapid eye movement (REM) sleep behavior disorder (RBD) is a disturbing parasomnia that manifests the loss of normal skeletal muscle atonia, excessive motor activity, and dream-enacting behaviors during the REM stage of sleep. The occurrence of RBD varies from 0.5% to 1.25% within the general population (1-4) and 1.06% in the sample of middle-to-older individuals (1). Moreover, evidence suggests that at least 50% of Parkinson's disease (PD) patients are estimated to experience RBD symptoms (5). Despite mounting evidence that the presence of RBD leads to a decrease in the sleep quality of PD patients, increases the risk of harming themselves and their bed companions, and worsens their cognitive function (6), the precise causal mechanisms still require additional investigation.

RBD is widely thought to be caused by pathology within the pontine nuclei of the brainstem (7). Generally, the glutamatergic neurons of the pontine sublaterodorsal nucleus (SLD), also called the subcoeruleus region, are considered to generate REM-related atonia. Glutamatergic SLD neurons increase firing in anticipation of REM sleep (REM-on cells), presumably together with others, and project to the inhibitory interneurons in ventromedial medulla (vMM) and the spinal cord, causing motor atonia (8-12). When the REM sleep circuit is damaged, it triggers the loss of normal REM sleep atonia and leads to RBD-like motor behaviors in humans and animals (11,13-19). The pedunculopontine nuclei (PPN), located in the upper brainstem, consist of dopaminergic, cholinergic, gamma-aminobutyric acid energetic (GABAergic), and glycinergic neurons. Animal experiments have found that PPN might disrupt the REM-tonic deficit circuit, leading to abnormal dystonia and hyperkinesia during the REM period (20,21). Population experiments have suggested that RBD might result from losing cholinergic tension in the PPN (22,23). Additionally, deep brain stimulation (DBS) targeting the PPN has been shown to increase sleep efficiency, improve REM stage sleep symptoms, and reduce arousals in PD patients (24). The substantia nigra compacta (SNc) dopaminergic neurons are considered a component of the REM sleep system involved in sleep regulation. Previous studies have shown that overexpression of α-synuclein in the SNc could alter hypotonia during REM sleep and significantly increase RBD events (25). Indeed, SNc merges with PPN, possibly through fiber projections to the SLD, and jointly participates in the REM-relaxation circuit and the REM stage generator circuit. However, a diffusion tensor imaging study did not find any differences in brainstem structures between PD patients with and without RBD (26,27). Another magnetic resonance spectroscopy study revealed no statistically significant differences in brainstem proton magnetic resonance spectroscopy parameters between PD patients with and without RBD (28). Moreover, a post-mortem analysis conducted on individuals with Lewy body disease discovered no discernible variations in the extent of neuronal degeneration or pathological accumulation of α-synuclein in the pontine tegmentum, irrespective of the symptoms of RBD during their lifetime (29). Meanwhile, a multicenter study of the transition from isolated RBD (iRBD) to synucleinopathy exposed that motor symptoms progressed the most throughout the follow-up and transformation of iRBD compared to non-motor symptoms such as cognitive abnormalities, olfactory disturbances, and sleep disorders (30). These pieces of evidence suggest that exclusive pathological changes in the brainstem may not be adequate to lead to RBD in PD. In fact, brainstem damage cannot account for the typically aggressive dream content exhibited by RBD patients, nor can it explain the higher severity of motor (31) and cognitive impairment (32) observed in PD patients with RBD (PD-RBD). There might be more extensive damage to the structure or function of the brain.

In reality, recent studies have revealed that RBD was implicated in structural and functional changes in the nigrostriatal, limbic system, cortex, and other multi-systemic neurodegenerative processes outside the brainstem (33). For example, a voxel-based morphometric approach found that both iRBD and PD patients with probable RBD (PD-pRBD) showed gray matter atrophy in temporal and occipital regions compared to healthy controls (HCs) (34). A functional magnetic resonance imaging (fMRI) study exhibited reduced functional connectivity (FC) in the temporal and parietal cortex of the brain in iRBD patients compared to the HCs (35). A metabolic imaging study showed that dopamine transporter density was significantly reduced in the anterior and posterior putamen and the

caudate nucleus in PD-pRBD patients compared to iRBD patients and HCs (36). Among the various neuronal injury mechanisms, the changes in FC of the cerebral cortex are gaining increasing attention. fMRI studies have uncovered that PD patients with RBD have significantly increased functional activity between the left cerebellum and bilateral occipital regions, bilateral supplementary motor area, and bilateral temporal regions while compared with PD patients without RBD (PD-nRBD) (37). Moreover, in the FC study, polysomnogram (PSG) confirmed that PD-RBD patients demonstrated a reduction in FC between the right superior occipital gyrus and the posterior regions (left fusiform gyrus, calcarine sulcus, and ipsilateral superior parietal gyrus) as opposed to those with PD-nRBD (38). A neuroelectrophysiological study using transcranial magnetic stimulation (TMS) manifested abnormalities in dopaminergic and GABA/glycinergic-mediated reticular and thalamocortical projections in iRBD patients (39). Accordingly, we legitimately hypothesize that PD-pRBD patients might also experience damaged connectivity within the entire functional network of the brain. Meanwhile, combined with different anatomic initial locations and propagation orientations of misfolded α-synuclein pathological changes (40), we intended to determine if the FC abnormalities in PD-pRBD patients also manifest inherent directional properties. However, to our best knowledge, few works have considered the node density alternations of internal network connections in PD-pRBD patients, and the directionality of brain network connectivity interruptions has not been mentioned.

Thus, we used a combination of graph-theoretical based degree centrality (DC) and Granger causality analysis (GCA) to explore the node density and directional changes of brain FC in PD patients with pRBD. DC metric quantifies the functional associations between a specific region (referred to as a node) and the remaining regions of the brain within the comprehensive connectivity matrix and represents the count of direct links for a given voxel in voxel-based graphs (41,42), which has been validated as an anomaly in PD and related complications (43-45). GCA can identify directional functional (causal) linkages using time series data, thus reflecting the characteristics of brain functional circuits and clarifying the causal relationship between different regions of the brain (46). Furthermore, we conducted the support vector machine (SVM) for inter-group evaluation of the classification performance based on regions that exhibited notable variations in DC. We present this article in accordance with the STROBE reporting checklist (available at https://qims.amegroups.com/article/view/10.21037/qims-24-1196/rc).

Methods

Cases

We enrolled 66 consecutive right-handed PD patients (female 28; male 38; mean age 59.8±8.8 years) from the outpatient department of the Neurology Department of the First Affiliated Hospital in Nanjing Medical University. The main requirements for inclusion in this study were: (I) compliance with the Movement Disorder Society clinical diagnostic criteria for PD (47); (II) having taken medicine steadily for at least 4 weeks. Our exclusion criteria for patients were as follows: (I) severe respiratory, circulatory, and organic brain disorders; (II) contraindications for magnetic resonance imaging (MRI); (III) dementia, depression, or any other neurological and psychiatric diseases; (IV) cognitive disorders [Mini-Mental State Examination (MMSE) scores <24]; and (V) excessive head motion. Meanwhile, 32 HCs who were similar in age, sex, and educational attainment were likewise recruited (female 12; male 20; mean age 62.3±6.2 years).

This study was conducted in accordance with the Declaration of Helsinki (as revised in 2013) and approved by the Ethics Committee of the First Affiliated Hospital of Nanjing Medical University (No. 2019-SRFA-094). All participants provided written informed consent prior to participating in the study and undergoing MRI procedures.

Clinical assessment

Probable RBD was screened based on the REM Sleep Behavior Disorder Screening Questionnaire (RBDSQ) with a cut-off score of 6 (48). PD patients with RBDSQ score ≥6 were classified as PD-pRBD (n=31), whereas those with RBDSQ score ≤3 were regarded as without pRBD (PD-npRBD, n=35). To mitigate possible misclassification, we removed blurred PD patients with RBDSQ scores of 4 and 5 (49). The RBDSQ, a 13-item questionnaire focused on the features of dreams and dream deductive behaviors, has been approved as a reliable measure for RBD (48,50-52). Furthermore, PD patients underwent other clinical evaluations during the drug-off state (without medication for at least 12 hours), which included Unified Parkinson's Disease Rating Scale III (UPDRS-III), the modified Hoehn and Yahr (H&Y) stage, MMSE scores, levodopa equivalent

daily dose (LEDD) (53), Hamilton Anxiety Rating Scale (HAMA), 24-item Hamilton Depression Rating Scale (HAMD-24), and Epworth Sleepiness Scale (ESS) (54).

MRI data acquisition

An image scanner, Siemens 3.0-Tesla MAGNETOM Verio whole-body scanner (Siemens Medical Solutions, Erlangen, Germany), was used to acquire images of PD patients in the drug-off stage and the HCs. Then, we utilized an eight-channel, phased-array head coil with foam padding and earplugs to minimize head motion and noise. We obtained the high-resolution three-dimensional (3D)-T1 structural images using a 3D volumetric magnetization prepared rapid gradient-echo (3D-MP-RAGE) sequence: repetition time (TR) =1,900 ms, echo time (TE) =2.95 ms, flip angle (FA) =9°, slice thickness =1 mm, slices =160, field of view (FOV) = 230×230 mm^2, matrix size =256×256, and voxel size =1×1×1 mm^3. We collected functional images with an echo-planar imaging (EPI) sequence: TR =2,000 ms, TE =21 ms, FA =90°, FOV =256×256 mm^2, in-plane matrix =64×64, slices =35, slice thickness =3 mm, slice gap =0 mm, voxel size =3×3×3 mm^3, total volumes =240. Notably, in the course of resting-state (RS)-fMRI scanning, patients were asked to remain relaxed, empty their brains, avoid movement, and not fall asleep. At last, no participant was reported to have fallen asleep during data acquisition.

MRI data preprocessing

The fMRI data went through preprocessing via DPABI software (http://www.restfmri.net/forum/dparsf). Detailed descriptions of these procedures have been provided in our previous publication (44). In brief, the process involves removing the first 10 time points and performing slice timing and head motion correction on the remaining 230 images. During this process, we excluded participants whose head motions exceeded 2.5 mm of translation or 2.5° of rotation. Afterward, the scalp structure was removed from the images, and 3D T1-weighted images were registered with the functional images. By applying the new segment and DARTEL techniques, the white matter (WM), gray matter (GM), and cerebrospinal fluid (CSF) were subdivided, followed by segmenting into the Montreal Institute of Neurology (MNI) nonlinear deformation space. Following spatial normalization, we employed a 6 mm full-width half-maximum Gaussian kernel for spatial smoothing. Finally, bandpass filtering (0.01–0.08 Hz) was performed, and linear trends were eliminated. Additionally, we eliminated several noise covariates during this process. Moreover, we computed each participant's average framewise displacement (FD) values and compared them among groups following preprocessing. The results indicated that the mean FD among the three groups was not statistically noteworthy (P=0.463).

Voxel-based DC calculation

Binary DC measures were performed on all preprocessed functional images using DPARSF. To obtain the graph for each participant, we calculated the Pearson correlation coefficient by computing the time series between a solitary voxel from the GM mask and all other voxels present within the brain. A Fisher-z transformation was then applied to the individual correlation matrices to improve normality. The Pearson correlation coefficient was thresholded at r>0.25 in order to eliminate possible spurious correlations (41,55). Subsequently, we performed spatial smoothing on the z-map using an isotropic 6 mm full-width half-maximum Gaussian kernel targeting to reduce errors in brain sulcus and gyrus structures after image standardization, increase data normality, and facilitate statistical analysis.

GCA analysis

The GCA was calculated using the RS-fMRI Data Analysis Toolkit (REST, http://www.restfmri.net). According to the MNI standard spatial coordinate system, the peak coordinate point [60, 6, 33] with significant differences in z-DC between PD subgroups was used as the seed point, and a sphere with a radius of 6 mm was used as the region of interest (ROI). A causal effect analysis was conducted based on the time series of each voxel and the seed point to describe the effective connectivity (EC) between voxels. In our research, the average time series of the right precentral gyrus was defined as the seed point time series x, and the time series of each voxel in the total brain was designated as y. A positive coefficient indicates that the activity of the right precentral gyrus exerted a causal influence on the activity in the region y in a congruent trajectory, whereas a negative coefficient indicates the opposite (46). Each seed point was subjected to two analyses: causal effect connectivity analysis (x to y) from the seed point to other voxels inside the entire brain and causal effect connectivity analysis (y to x) from the whole brain voxel to the seed region. In this way, GCA maps from the right precentral gyrus to the totality of the

brain and from the whole brain to the right precentral gyrus were produced for each participant. Finally, we transformed the GCA maps with Fisher-z to obtain z-valued GCA maps.

SVM classification analysis

SVM classification (LIBSVM, https://www.csie.ntu.edu.tw/~cjlin/libsvm/) was employed to identify the minimum separated hyperplane in a high-dimensional space for data classification. Generally, two steps are involved in the classification process: training and testing. Firstly, the regional DC metrics in the right precentral gyrus selected as features were screened into the SVM model to establish the hyperplane. Next, the training dataset and test dataset were divided in a ratio of 8:2. Then, we applied the radial basis function (RBF) kernel in the study. Based on the training data, c (penalty coefficient) and g (gamma) were selected as the two most desirable parameters by the grid search method. Additionally, the optimal hyperplane generated from the training data was applied to the newly generated test dataset to evaluate the classification algorithm's performance. With the use of the "leave-one-out" cross-validation method (56), the accuracy, sensitivity, and specificity yielded the highest results. Lastly, we calculated the area under the curve (AUC) to assess the established model's predictive power.

Statistical analysis

All statistical analyses were carried out utilizing the software SPSS 25.0 (IBM Corp., Armonk, NY, USA). Following the Shapiro-Wilk test to determine the normality of the data, the age differences among the three groups of participants were analyzed using the one-way analysis of variance (ANOVA). Based on a two-sample *t*-test, the differences in onset age, UPDRS-III, and the HAMA between two PD groups were examined. We compared sex, initial side of onset of motor symptoms, education, the mean FD, MMSE, and RBDSQ among the three groups using the chi-square and Kruskal-Wallis tests since these variables were not normally distributed. The Mann-Whitney *U* test was applied to analyze the disease duration, H&Y stages, LEDD, HAMD-24, and the ESS scores between PD patients with pRBD versus those without pRBD due to the non-normality of the materials. A significance level of P<0.05 was set for sociodemographic and clinical data.

The DPABI statistical analysis package was adopted to calculate and analyze the z-DC values for all groups. We detected significant variations in z-DC between the three groups deploying the ANOVA approach, coupled with sex, age, and education covariates. The ANOVA results were subsequently analyzed by a two-sample post hoc *t*-test with covariates mentioned before for each pair of groups. All statistical significance complied with Gaussian random field (GRF) correction with voxel-level P<0.001 and a cluster-level P<0.05 as multiple comparison correction (two-tailed).

Additionally, we performed GCA analysis on the whole brain utilizing brain regions exhibiting varying z-DC values among the subgroups of individuals with PD. A two-sample *t*-test with age, sex, and education level as covariates was then used to compare the Granger causality (GC) maps of two PD groups from the seed region to the whole brain (x to y), combined with an uncorrected voxel-level P<0.01 and a GRF-corrected cluster-level P<0.05 under the causal effects mask, respectively. Meanwhile, the GC maps from the complete brain to the seed region (y to x) followed similar statistical principles.

Finally, Spearman's rank correlations were used to measure correlations between the RBDSQ scores and the average z-DC values in the PD-pRBD patients, as well as EC modifications. Furthermore, we inspected Pearson's correlation between the UPDRS-III scores and the mean z-DC and EC values in PD-pRBD patients. Moreover, we employed Spearman's correlation analysis to perform statistical analyses of the relationship between RBD symptoms and depression and cognition in PD-pRBD patients.

Results

Demographic and clinical characteristics

Table 1 summarizes the clinical characteristics of PD-pRBD, PD-npRBD, and HCs groups. Initially, no statistically discernible variations were spotted among the three groups concerning age, sex, education, mean FD, and MMSE scores (P>0.05). Besides, neither disease duration, age at onset, initial side of onset of motor symptoms, UPDRS-III scores, modified H&Y stages, LEDD, HAMA, nor HAMD-24 scores varied between subgroups (P>0.05). However, PD-pRBD patients displayed significantly elevated RBDSQ and ESS scores as opposed to patients of PD-npRBD (P<0.05).

DC analysis

DC evaluations showed that the z-DC values of the right

Table 1 Demographic and clinical characteristics of all subjects

Items	PD-pRBD (n=31)	PD-npRBD (n=35)	HCs (n=32)	P value	Post hoc (Bonferroni)
Age (years)	61.1±7.3	58.5±9.9	62.3±6.2	0.153[a]	
Sex (female/male)	10/21	18/17	12/20	0.257[b]	
Education (years)	9.0 (3.0)	9.0 (3.0)	12.0 (4.8)	0.196[c]	
Disease duration (years)	7.0 (5.0)	6.0 (4.0)	NA	0.708[d]	
Mean FD	0.1 (0.1)	0.1 (0.1)	0.1 (0.1)	0.463[c]	
MMSE	29.0 (1.0)	29.0 (2.0)	30.0 (1.8)	0.078[c]	
Age at onset (years)	54.0±7.6	50.6±11.0	NA	0.157[e]	
Initial side of onset of motor symptoms (R/L)	6/25	9/26	NA	0.538[b]	
UPDRS-III (OFF state)	33.9±11.9	29.2±11.9	NA	0.114[e]	
H&Y stages	2.0 (1.0)	2.0 (1.5)	NA	0.095[d]	
LEDD (mg/day)	693.8 (475)	675.0 (275)	NA	0.969[d]	
HAMA	6.8±2.9	6.5±3.3	NA	0.709[e]	
HAMD-24	6.0 (2.0)	6.0 (2.0)	NA	0.474[d]	
ESS	8.0 (7.0)	5.0 (5.0)	NA	0.005[d]	
RBDSQ	10.0 (4.0)	2.0 (3.0)	1.0 (2.0)	<0.001[c]	<0.001*[f], <0.001*[g], 0.519[h]

Data are presented as mean ± standard deviation, median (interquartile range), or number. [a], one-way analysis of variance; [b], Chi-square test; [c], Kruskal-Wallis test; [d], Mann-Whitney *U* test; [e], two-sample *t*-test; *, P<0.05 was considered significant; [f], P values between PD-pRBD and PD-npRBD groups; [g], P values between PD-pRBD and HCs groups; [h], P values between PD-npRBD and HCs groups. PD, Parkinson's disease; PD-pRBD, Parkinson's disease with probable rapid eye movement sleep behavior disorders; PD-npRBD, Parkinson's disease without probable rapid eye movement sleep behavior disorders; HCs, healthy controls; FD, framewise displacement; MMSE, Mini Mental State Examination; R, right; L, left; UPDRS, Unified Parkinson's Disease Rating Scale; OFF, drug-off period; H&Y stage, Hoehn and Yahr stage; LEDD, levodopa equivalent daily dose; HAMA, Hamilton Anxiety Scale; HAMD-24, Hamilton Depression Scale-24; ESS, Epworth Sleepiness Scale; RBDSQ, Rapid Eye Movement Sleep Behavior Disorder Screening Questionnaire; NA, not applicable.

precentral gyrus decreased in PD-pRBD patients weighed against those in PD-npRBD group (*Figure 1*, *Table 2*). Along with the right precentral gyrus, PD-pRBD also exhibited lower z-DC values in the right postcentral gyrus and the superior parietal lobule than the HCs. Additionally, z-DC in the right superior parietal lobule was significantly reduced in the PD-npRBD group in comparison to the HCs group. Notably, the z-DC values of the right precentral gyrus in PD-pRBD patients were negatively correlated to the RBDSQ scores (*Figure 2A*), whereas there was no correlation with UPDRS-III scores (*Figure 2B*). Moreover, we did not discover a correlation between RBDSQ scores and MMSE (*Figure 2C*) or HAMD-24 scores (*Figure 2D*).

GCA analysis

There was a reduction in EC from the right precentral gyrus to the right caudate nucleus in PD-pRBD patients contrasted with PD-npRBD patients (*Figures 3*,*4*, *Table 3*). Further, correlation analysis demonstrated that EC values from the right precentral gyrus to the ipsilateral caudate nucleus were negatively related to the RBDSQ scores (*Figure 5A*), whereas there was no correlation with UPDRS-III scores (*Figure 5B*). In contrast, no statistically significant disparity in EC was noticed between the PD groups from the whole brain to the right precentral gyrus.

SVM classification analysis

SVM analyses were performed to examine whether z-DC values in the right precentral gyrus could be valuable for identifying PD-pRBD and PD-npRBD patients. The z-DC values in the right precentral gyrus demonstrated a sensitivity of 66.67%, a specificity of 100%, and an AUC of 0.905 for

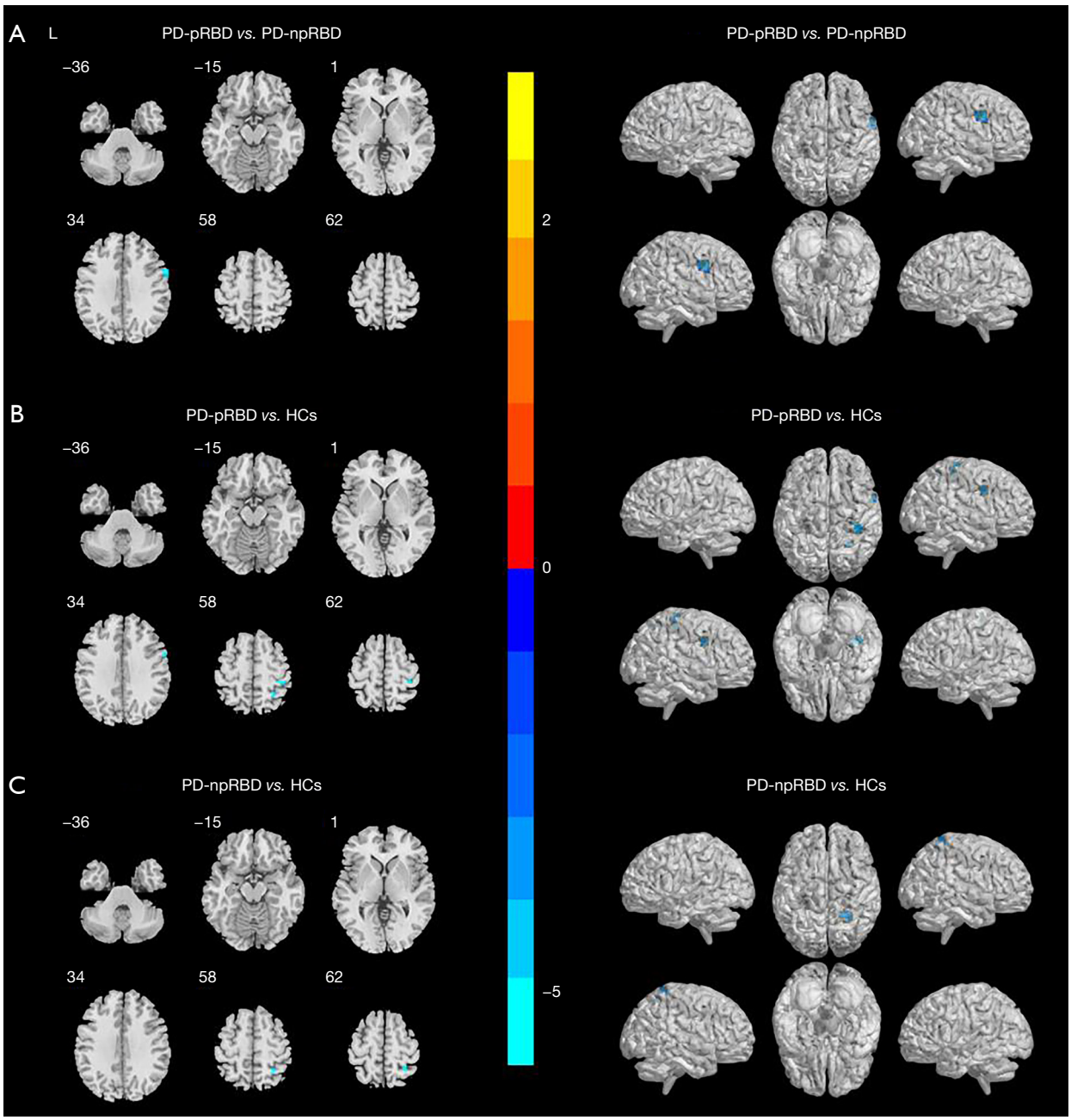

Figure 1 Significant differences of DC result maps among three groups: PD-pRBD, PD-npRBD, and HCs. Statistical threshold was displayed at voxel-level P value <0.001, Gaussian random field corrected, cluster-level P value <0.05. Cool colors represent significantly decreased DC. (A) Differences between PD-pRBD and PD-npRBD; (B) differences between PD-pRBD and HCs; (C) differences between PD-npRBD and HCs. L, left; PD, Parkinson's disease; PD-pRBD, Parkinson's disease with probable rapid eye movement sleep behavior disorders; PD-npRBD, Parkinson's disease without probable rapid eye movement sleep behavior disorders; HCs, healthy controls; DC, degree centrality.

Table 2 Brain regions with abnormal DC between the groups

Brain regions (AAL)	Peak MNI coordinates			Number of voxels	Peak t value
	x	y	z		
PD-pRBD *vs.* PD-npRBD					
Precentral_R	60	6	33	28	–5.7984
PD-pRBD *vs.* HCs					
Precentral_R	57	6	33	11	–4.8712
Postcentral_R	39	–33	57	23	–5.3341
Parietal_Sup_R	27	–51	57	9	–4.5480
PD-npRBD *vs.* HCs					
Parietal_Sup_R	24	–48	69	24	–4.6313

The significance of post-hoc *t*-tests was set at voxel-level P<0.001, cluster-level P<0.05, corrected by Gaussian random field, determined by Monte Carlo simulation for multiple comparisons. Negative T value signifies the regions in which the former group had lower DC values than the latter group. DC, degree centrality; AAL, anatomical automatic labeling; MNI, Montreal Neurological Institute; PD-pRBD, Parkinson's disease with probable rapid eye movement sleep behavior disorders; PD-npRBD, Parkinson's disease without probable rapid eye movement sleep behavior disorders; HCs, healthy controls; R, right.

discriminating PD-pRBD from PD-npRBD (*Figure 6*). For more details, please refer to (Figure S1, Table S1).

Discussion

In the current research, we characterized variations in brain internal connectivity patterns in PD patients with pRBD by applying DC and GCA analyses. Importantly, our SVM method further emphasized that the mean z-DC values in the abnormally altered DC regions can assume the role of imaging peculiarities in PD-pRBD patients. More concretely, we observed that PD-pRBD patients had decreased z-DC values in the right precentral gyrus compared to PD-npRBD patients (*Figure 1*, *Table 2*). Secondly, GCA analysis with the right precentral gyrus as a seed point indicated that PD-pRBD patients exhibited reduced EC values from the right precentral gyrus to the right caudate nucleus, relative to individuals with PD-npRBD (*Figures 3*,*4*, *Table 3*). However, PD-pRBD patients did not display any alternation in EC from the whole brain to the right precentral gyrus. Thirdly, both DC and EC changes in the PD-pRBD group negatively correlated with RBDSQ scores (*Figure 2A*, *Figure 5A*). Further, the SVM results confirmed that the z-DC values pertaining to the right precentral gyrus might operate as an advantageous neuroimaging tool for distinguishing PD-pRBD patients (*Figure 6*). Notably, we observed no relationship between the severity of the RBD and the MMSE or HAMD-24 scores (*Figure 2C*,*2D*). We hypothesized that this might be due to the purposeful exclusion of patients with cognitive and depressive disorders from the patient recruitment procedure.

Our findings demonstrated that PD-pRBD patients had lower z-DC values in the right precentral gyrus than the PD-npRBD and HCs groups, indicating the vitiated node density in the precentral motor cortex and its impaired brain information transmission function in PD patients with pRBD. As is widely acknowledged, the precentral gyrus, occupied predominantly by the primary motor cortex (M1), controls the autonomous movement of the whole body with other brain regions. According to prior studies, activity attenuation of the motor cortex, including the M1, may lead to movement disorders (57) and partly account for RBD patients' poor voluntary movement control (58). Such an interpretation was supported by an RS-fMRI study (59), showing that PD patients with PSG-confirmed RBD presented decreased amplitude of low-frequency fluctuations (ALFF) values in the M1 extending to the premotor cortex compared with PD patients without RBD. In fact, even in the early stage of RBD, iRBD patients have been documented to exhibit reduced local cerebral perfusion in the motor cortex (including the M1) (58), thinning motor cortical thickness (60), and decreased FC between the motor and somatosensory cortex (61) compared to HCs. Meanwhile, PD patients with RBD have been shown to manifest much worse motor symptoms when compared to those without RBD, and were associated with higher levodopa dosage for antiparkinsonian therapy (31). Thus, our findings and existing literature suggest that FC interruption in the precentral motor cortex may cause poor voluntary motor control, which was linked to PD-pRBD patients. Moreover, our correlation analysis further revealed that the worse the node density of the right precentral gyrus, the more severe pRBD symptoms in PD patients. Additionally, as a high-resolution machine learning method, our SVM supported a potential value of the z-DC in the right precentral gyrus for distinguishing PD-pRBD from PD-npRBD and HCs groups, which may be a latent trait of PD patients with pRBD. Meanwhile, the motor cortex is also believed to be a generator of REM sleep movements (62,63), which undergoes brief functional reconstruction during REM sleep. Concretely, the M1 temporarily

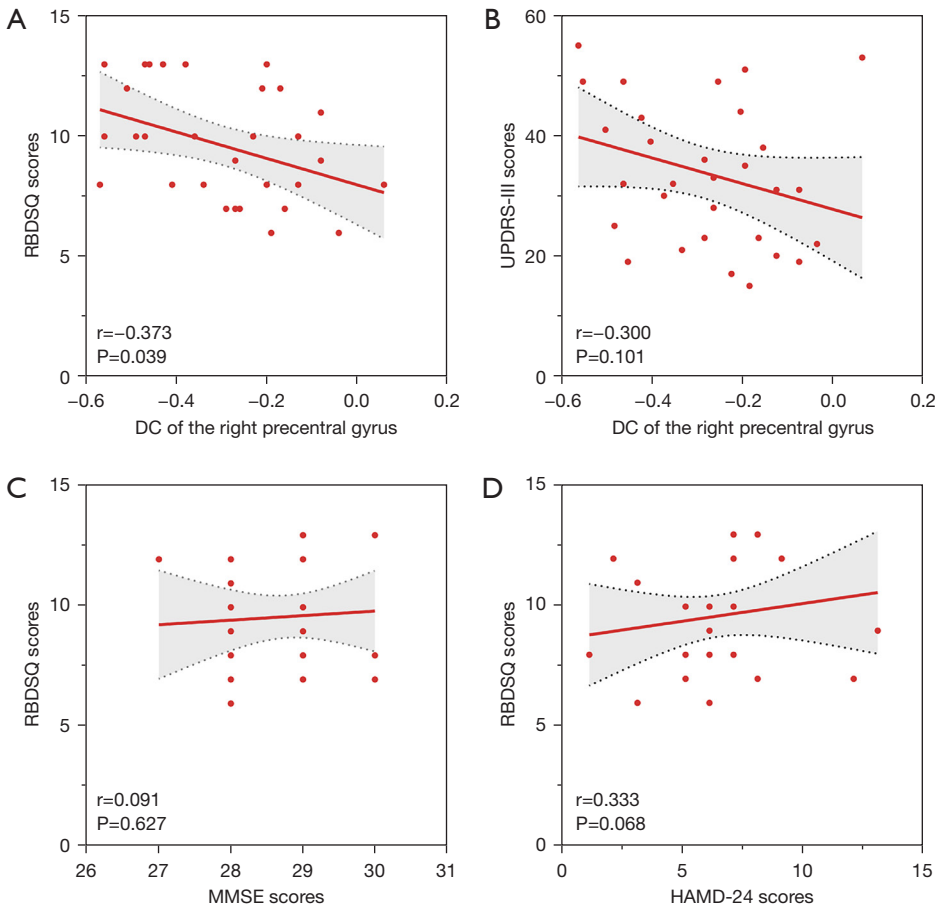

Figure 2 Correlation analysis results during the drug-off state within PD-pRBD patients. (A) Correlations between z-DC values and RBDSQ scores in right precentral gyrus during the drug-off state of PD-pRBD patients. Scatterplots presented a significant negative correlation (P<0.05). (B) Correlations between z-DC values and UPDRS-III scores in right precentral gyrus during the drug-off state of PD-pRBD patients. Scatterplots presented no significant correlation (P>0.05). (C) Correlations between RBDSQ and MMSE scores in PD-pRBD patients during the drug-off state. Scatterplots presented no significant correlation (P>0.05). (D) Correlations between RBDSQ and HAMD-24 scores in PD-pRBD patients during the drug-off state. Scatterplots presented no significant correlation (P>0.05). DC, degree centrality; RBDSQ, rapid eye movement sleep behavior disorder screening questionnaire; UPDRS, Unified Parkinson's disease rating scale; MMSE, Mini Mental State Examination; HAMD-24, Hamilton Depression Scale-24; PD-pRBD, Parkinson's disease with probable rapid eye movement sleep behavior disorders.

activates during RBD onset, bypasses the basal ganglia's filtering and smoothing, and ultimately transmits the signal to the lower motor neurons (63). This is consistent with the typical motor symptoms of PD patients with RBD: although patients have poor motor performance due to asymmetric parkinsonism while awake, they report rapid, coordinated, and smooth movements as well as improved speech and facial expressions during night RBD episodes, and patients tend to move their disabled side more frequently. However, this phenomenon might be caused by the depth limitation of the PSG to monitor cortical electrical activity. Functional abnormalities in subcortical electrical activity would be missed because of the limited depth of electrode monitoring. Overall, although we currently cannot explicate the specific paradoxical mechanism between the impaired node information transmission in the precentral motor cortex of PD-pRBD patients and the transient activation of this brain region during RBD attacks, our observations provide evidence that the precentral motor cortex presumably engages in the RBD inherent mechanism that underlies PD.

To elucidate the directional issue of node density alternations in the right precentral gyrus between PD

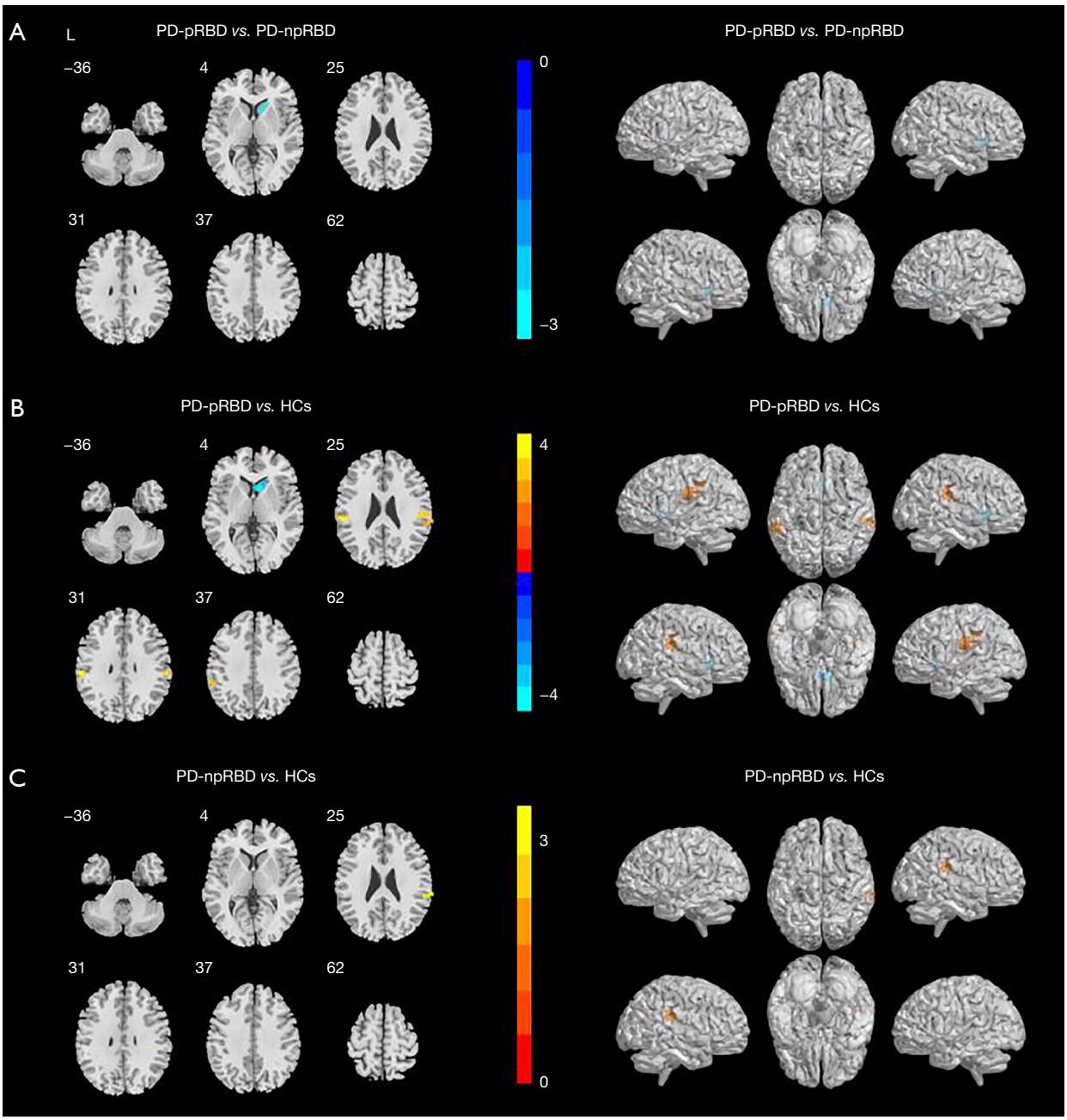

Figure 3 Significant differences of EC result maps among three groups: PD-pRBD, PD-npRBD, and HCs. Statistical threshold was displayed at voxel-level P value <0.01, Gaussian random field corrected, cluster-level P value <0.05. Cool colors represent significantly decreased EC, whereas warm colors represent the opposite. (A) differences between PD-pRBD and PD-npRBD; (B) differences between PD-pRBD and HCs; (C) differences between PD-npRBD and HCs. L, left; PD, Parkinson's disease; PD-pRBD, Parkinson's disease with probable rapid eye movement sleep behavior disorders; PD-npRBD, Parkinson's disease without probable rapid eye movement sleep behavior disorders; HCs, healthy controls; EC, effective connectivity.

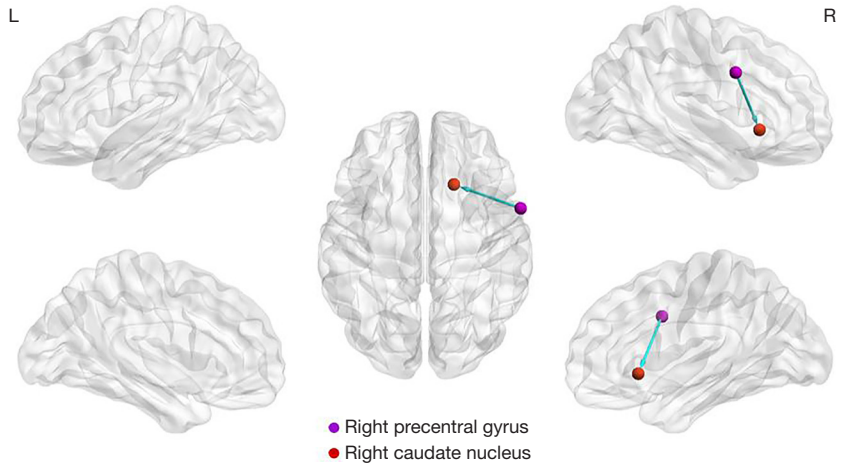

Figure 4 Sketch map of the between-group differences in causal connectivity: PD-pRBD versus PD-npRBD. The arrow of the significant causal paths represents the direction of the information flow. The seed point in the right precentral gyrus [60, 6, 33] as the purple ball, and the red ball represents the right caudate nucleus. L, left; R, right; PD-pRBD, Parkinson's disease with probable rapid eye movement sleep behavior disorders; PD-npRBD, Parkinson's disease without probable rapid eye movement sleep behavior disorders.

Table 3 Brain regions with abnormal EC between the groups

Brain regions (AAL)	Peak MNI coordinates			Number of voxels	Peak t value
	x	y	z		
Outflow from the right precentral gyrus to whole brain					
PD-pRBD *vs.* PD-npRBD					
Caudate_R	18	21	−3	35	−3.1636
PD-pRBD *vs.* HCs					
Caudate_R	9	15	3	93	−4.2504
SupraMarginal_R	54	−18	24	57	3.9452
SupraMarginal_L	−57	−27	27	55	4.5027
PD-npRBD *vs.* HCs					
SupraMarginal_R	66	−33	24	22	3.3996

The significance of post-hoc *t*-tests was set at voxel-level P<0.01, cluster-level P<0.05, corrected by Gaussian random field, determined by Monte Carlo simulation for multiple comparisons. Negative *t* value signifies the regions in which the former group had lower EC values than the latter group, whereas positive t value indicates the opposite. EC, effective connectivity; AAL, anatomical automatic labeling; MNI, Montreal Neurological Institute; PD-pRBD, Parkinson's disease with probable rapid eye movement sleep behavior disorders; PD-npRBD, Parkinson's disease without probable rapid eye movement sleep behavior disorders; HCs, healthy controls; R, right; L, left.

subgroups, we conducted inter-group EC analyses using the right precentral gyrus as the seed brain region. EC represents the direct causal relationship between two brain regions, offering insight towards the neuropathological processes underlying the functional architecture within the brain (64,65). GCA can accomplish EC analysis by recognizing directed functional interactions in time series. In the present investigation, we ascertained a significantly decreased EC from the right precentral gyrus to the right caudate nucleus between PD subgroups. The caudate nuclei, as a crucial component of the striatum in the basal ganglia, are thought to be involved in motor regulation (66) and cognitive functions (67,68), and play a vital position in the sleep-wake cycle. For example, observation of cats with the caudate nucleus ablated revealed permanent hyperactivity with markedly decreased REM sleep time (69), suggesting the importance of the caudate nucleus in REM sleep. Actually, caudate nucleus abnormalities have been extensively documented as early as the prodromal state of alpha-synucleinopathies, also called the iRBD stage (60,70). For instance, an MRI study reported that video PSG confirmed iRBD patients reported a decrement in the volume of the right caudate nucleus compared with HCs. Furthermore, a negative correlation was found between global iron deposition in the left caudate nucleus

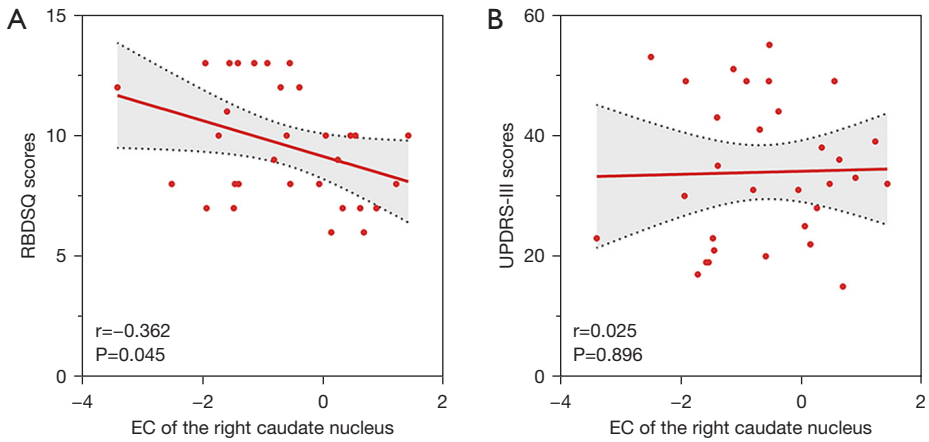

Figure 5 Correlation analysis results during the drug-off state within PD-pRBD patients. (A) Correlations between EC values and RBDSQ scores in right caudate nucleus during the drug-off state of PD-pRBD patients. Scatterplots presented a significant negative correlation (P=0.045). (B) Correlations between EC values and UPDRS-III scores in right caudate nucleus during the drug-off state of PD-pRBD patients. Scatterplots presented no significant correlation (P=0.896). RBDSQ, rapid eye movement sleep behavior disorder screening questionnaire; EC, effective connectivity; UPDRS, Unified Parkinson's disease rating scale; PD-pRBD, Parkinson's disease with probable rapid eye movement sleep behavior disorders.

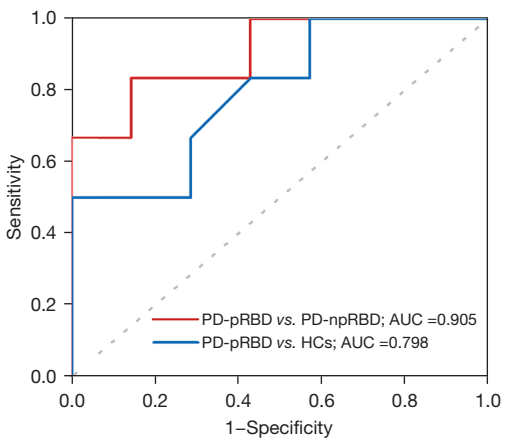

Figure 6 ROC analyses for differentiating different groups through SVM. The results revealed that the z-DC values of the right precentral gyrus showed significant potential as an indicator for separating PD-pRBD from PD-npRBD (AUC =0.905). The z-DC values of the right precentral gyrus showed moderate potential as an indicator for separating PD-pRBD from the HCs (AUC =0.798). See Table S1 and Figure S1 for more details. ROC, receiver operating characteristic; PD, Parkinson's disease; PD-pRBD, Parkinson's disease with probable rapid eye movement sleep behavior disorders; PD-npRBD, Parkinson's disease without probable rapid eye movement sleep behavior disorders; HCs, healthy controls; AUC, area under the curve; DC, degree centrality; SVM, support vector machine.

and poor motor performance in iRBD patients (70). In line with this, several neuroimaging studies have linked the presence of RBD without PSG confirmation in PD with more accelerating dopaminergic denervation (71) and volume decline (72) in the caudate nucleus as time passes. Similar findings from neuroelectrophysiological research have indicated that RBD may regulate the central nervous system's general neurochemical balance, influencing the projections of upstream pathways that go to the cortex, such as the reticular and thalamocortical projections. TMS therapies may reduce sleep symptoms by adjusting the intensity of cortical and subcortical connectivity and the synaptic plasticity between different brain regions (73,74). These research results indirectly match those of our study: a negative causal influence from the right precentral gyrus to the right caudate nucleus. According to a previous study, the caudate nucleus participates in correction movements for efferent motor and afferent sensory mismatches (75). Thus, we speculated that when the precentral motor cortex in PD-pRBD patients experienced dysfunction, the damaged caudate nucleus could not correct their defective motor commands, resulting in poor motor performance. Moreover, it also supported the hypothesis during the RBD attack that the precentral gyrus was temporarily functional reconstruction and transmitted directly through the pyramidal tract instead of the damaged caudate striatum

system. Our results also exposed a negative relationship between RBDSQ scores and the mean EC from the right precentral gyrus to the caudate nucleus. In other words, the more severe the symptoms of RBD in PD, the worse the interruption of EC from the precentral motor cortex to the ipsilateral caudate nucleus. This may indicate that damage to the motor cortex-striatal network and loss of FC were related to the pRBD of PD patients.

Another noteworthy finding was that PD-pRBD patients displayed lower z-DC values in the right postcentral gyrus than HCs, indicating decreased node density and message transfer function in the right postcentral somatosensory region. In this regard, structural MRI studies about iRBD have reported that iRBD patients confirmed by video PSG had decreased GM volume (76) and cortical thinning (77) compared with the HCs. An fMRI study using independent component analysis discovered that compared with the HCs group, iRBD patients diagnosed with PSG had not only reduced striatal-prefrontal FC in the executive-control network (ECN) but also diminished motor and somatosensory cortex FC in the sensory-motor network (SMN) (61). These studies summarized together that RBD patients without obvious clinical movement disorders already have abnormal brain structures and functions related to the movement and sensation regions. Similarly, a structural MRI study (27) revealed that PD patients with PSG-confirmed RBD possessed lower GM volume in the postcentral gyrus compared to HCs, whereas no significant difference was reported in comparison with PD-nRBD. These results align with our research results. So far, despite multiple reports of precentral gyrus impairment and dysfunction in RBD-related studies, there are currently few descriptions and speculations on its specific mechanisms. Morphological analyses of brain MRI in PD patients with concomitant sleep disorders have strongly linked cortical surface reduction of the right postcentral gyrus to PD patients with frequent distressful dreams (78), suggesting that the right postcentral gyrus might be relevant to poor dreams in PD patients. In this regard, RBD patients generally experience unpleasant, angry, and fearful nightmares (79,80) and even violent nocturnal dream performances. Therefore, we inferred rationally that FC disorders in the postcentral gyrus may be associated with unpleasant dreams among PD patients with pRBD. However, our PD subgroups did not display any DC abnormalities in the postcentral gyrus, possibly indicating that the diminished z-DC values in the postcentral gyrus may not be unique to RBD. In the future, more large-scale, prospective longitudinal investigations are expected to enlighten the pathological basis of PD-RBD further.

Surprisingly, our DC analysis for all three groups discovered the results chiefly situated in the right hemisphere of the brain, which was attributed to the majority of PD patients (51/66) experiencing severe motor symptoms and the onset of disease on the left side. Therefore, the brain's right hemisphere was more severely damaged according to the principle of contralateral brain control. Our findings matched previous studies (81,82), indicating asymmetric neurodegenerative alternations in the brain regions that dominate the affected side (83).

Our study has some limitations. First, we used RBDSQ scores rather than gold-standard PSG to determine the RBD status of PD patients. Although we adopted relatively rigorous RBDSQ cut-off values for grouping (49), we could not wholly eliminate grouping uncertainty. Second, we should acknowledge that our cases had not been entirely free of interference from drugs. However, we collected all data during the drug-off stage, and dopaminergic medications were comparable between our PD subgroups. If possible, future studies should focus on early drug-naïve PD patients with or without RBD to better validate this claim. Third, the comparatively small sample size impeded our analysis of functional differences in specific brain regions. Fourth, we solely executed cross-sectional analyses and did not apply any external intervention, such as using repetitive transcranial magnetic stimulation to intervene in M1 for validation. Therefore, it is necessary to expand the sample size and conduct interventional longitudinal studies in the future. Fifth, our study only elaborated the mechanism of PD patients with RBD from the perspective of MRI, which was relatively restricted from the perspective of blood oxygen level. In the future, we might consider combining molecular imaging such as single-photon emission computed tomography (SPECT) and positron emission tomography (PET) to explore the pathogenic mechanism of PD-pRBD from a multimodal and multifaceted perspective. Nevertheless, our study implemented modern analytical techniques, including machine learning and graph theory analysis, to better grasp the pathogenic impact in PD with RBD patients. Meanwhile, our findings provide new imaging markers for PD patients with RBD, facilitating early diagnosis and management of the disease.

Conclusions

Collectively, in this study, PD-pRBD patients had abnormal z-DC values in the right precentral gyrus compared

with PD-npRBD patients, and the aberrant EC from the right precentral gyrus to the right caudate nucleus might contribute to PD-pRBD pathogenesis. Besides, we identified that the z-DC values in the right precentral gyrus may be a potential imaging marker for PD-pRBD. In summary, our findings uncovered a malfunctioning EC pattern of the precentral motor cortex to the striatum of the caudate nucleus, providing novel insight into the pathophysiology of RBD in PD.

Acknowledgments

We are grateful to all of the participants for their cooperation and support in our study.
Funding: This work was supported by the National Natural Science Foundation of China (Nos. 82271273 and 81671258).

Footnote

Reporting Checklist: The authors have completed the STROBE reporting checklist. Available at https://qims.amegroups.com/article/view/10.21037/qims-24-1196/rc

Conflicts of Interest: All authors have completed the ICMJE uniform disclosure form (available at https://qims.amegroups.com/article/view/10.21037/qims-24-1196/coif). The authors have no conflicts of interest to declare.

Ethical Statement: The authors are accountable for all aspects of the work in ensuring that questions related to the accuracy or integrity of any part of the work are appropriately investigated and resolved. This study was conducted in accordance with the Declaration of Helsinki (as revised in 2013) and was approved by the Ethics Committee of The First Affiliated Hospital of Nanjing Medical University (No. 2019-SRFA-094). All participants provided written informed consent prior to participating in the study and undergoing MRI procedures.

References

1. Haba-Rubio J, Frauscher B, Marques-Vidal P, Toriel J, Tobback N, Andries D, Preisig M, Vollenweider P, Postuma R, Heinzer R. Prevalence and determinants of rapid eye movement sleep behavior disorder in the general population. Sleep 2018;41:zsx197.
2. Kang SH, Yoon IY, Lee SD, Han JW, Kim TH, Kim KW. REM sleep behavior disorder in the Korean elderly population: prevalence and clinical characteristics. Sleep 2013;36:1147-52.
3. Sasai-Sakuma T, Takeuchi N, Asai Y, Inoue Y, Inoue Y. Prevalence and clinical characteristics of REM sleep behavior disorder in Japanese elderly people. Sleep 2020;43:zsaa024.
4. Sateia MJ. International classification of sleep disorders-third edition: highlights and modifications. Chest 2014;146:1387-94.
5. Yousaf T, Pagano G, Wilson H, Politis M. Neuroimaging of Sleep Disturbances in Movement Disorders. Front Neurol 2018;9:767.
6. Postuma RB, Bertrand JA, Montplaisir J, Desjardins C, Vendette M, Rios Romenets S, Panisset M, Gagnon JF. Rapid eye movement sleep behavior disorder and risk of dementia in Parkinson's disease: a prospective study. Mov Disord 2012;27:720-6.
7. Boeve BF. REM sleep behavior disorder: Updated review of the core features, the REM sleep behavior disorder-neurodegenerative disease association, evolving concepts, controversies, and future directions. Ann N Y Acad Sci 2010;1184:15-54.
8. Karlsson KA, Gall AJ, Mohns EJ, Seelke AM, Blumberg MS. The neural substrates of infant sleep in rats. PLoS Biol 2005;3:e143.
9. Krenzer M, Lu J, Mayer G, Oertel W. From bench to bed: putative animal models of REM sleep behavior disorder (RBD). J Neural Transm (Vienna) 2013;120:683-8.
10. Lai YY, Siegel JM. Pontomedullary glutamate receptors mediating locomotion and muscle tone suppression. J Neurosci 1991;11:2931-7.
11. Lu J, Sherman D, Devor M, Saper CB. A putative flip-flop switch for control of REM sleep. Nature 2006;441:589-94.
12. Onoe H, Sakai K. Kainate receptors: a novel mechanism in paradoxical (REM) sleep generation. Neuroreport 1995;6:353-6.
13. Boissard R, Gervasoni D, Schmidt MH, Barbagli B, Fort P, Luppi PH. The rat ponto-medullary network responsible for paradoxical sleep onset and maintenance: a combined

microinjection and functional neuroanatomical study. Eur J Neurosci 2002;16:1959-73.
14. Henley K, Morrison AR. A re-evaluation of the effects of lesions of the pontine tegmentum and locus coeruleus on phenomena of paradoxical sleep in the cat. Acta Neurobiol Exp (Wars) 1974;34:215-32.
15. Mouret J, Delorme F, Jouvet M. Lesions of the pontine tegmentum and sleep in rats. C R Seances Soc Biol Fil 1967;161:1603-6.
16. Peever J, Fuller PM. The Biology of REM Sleep. Curr Biol 2017;27:R1237-48.
17. Provini F, Vetrugno R, Pastorelli F, Lombardi C, Plazzi G, Marliani AF, Lugaresi E, Montagna P. Status dissociatus after surgery for tegmental ponto-mesencephalic cavernoma: a state-dependent disorder of motor control during sleep. Mov Disord 2004;19:719-23.
18. Valencia Garcia S, Libourel PA, Lazarus M, Grassi D, Luppi PH, Fort P. Genetic inactivation of glutamate neurons in the rat sublaterodorsal tegmental nucleus recapitulates REM sleep behaviour disorder. Brain 2017;140:414-28.
19. Zambelis T, Paparrigopoulos T, Soldatos CR. REM sleep behaviour disorder associated with a neurinoma of the left pontocerebellar angle. J Neurol Neurosurg Psychiatry 2002;72:821-2.
20. Schenck CH, Mahowald MW. REM sleep behavior disorder: clinical, developmental, and neuroscience perspectives 16 years after its formal identification in SLEEP. Sleep 2002;25:120-38.
21. Kohlmeier KA, Burns J, Reiner PB, Semba K. Substance P in the descending cholinergic projection to REM sleep-induction regions of the rat pontine reticular formation: anatomical and electrophysiological analyses. Eur J Neurosci 2002;15:176-96.
22. Ringman JM, Simmons JH. Treatment of REM sleep behavior disorder with donepezil: a report of three cases. Neurology 2000;55:870-1.
23. Chambers N E, Lanza K, Bishop C. Pedunculopontine Nucleus Degeneration Contributes to Both Motor and Non-Motor Symptoms of Parkinson's Disease. Front Pharmacol 2020; 10:1494.
24. Romigi A, Placidi F, Peppe A, Pierantozzi M, Izzi F, Brusa L, Galati S, Moschella V, Marciani MG, Mazzone P, Stanzione P, Stefani A. Pedunculopontine nucleus stimulation influences REM sleep in Parkinson's disease. Eur J Neurol 2008;15:e64-5. Erratum in: Eur J Neurol 2008;15:e57.
25. Dautan D, Paslawski W, Montejo SG, Doyon DC, Marangiu R, Kaplitt M G, Chen R, Dawson VL, Zhang X, Dawson TM, Svenningsson P. Gut-Initiated Alpha Synuclein Fibrils Drive Parkinson's Disease Phenotypes: Temporal Mapping of non-Motor Symptoms and REM Sleep Behavior Disorder.bioRxiv [Preprint] 2024;26:590542.
26. Ford AH, Duncan GW, Firbank MJ, Yarnall AJ, Khoo TK, Burn DJ, O'Brien JT. Rapid eye movement sleep behavior disorder in Parkinson's disease: magnetic resonance imaging study. Mov Disord 2013;28:832-6.
27. Lim JS, Shin SA, Lee JY, Nam H, Lee JY, Kim YK. Neural substrates of rapid eye movement sleep behavior disorder in Parkinson's disease. Parkinsonism Relat Disord 2016;23:31-6.
28. Hanoglu L, Ozer F, Meral H, Dincer A. Brainstem 1H-MR spectroscopy in patients with Parkinson's disease with REM sleep behavior disorder and IPD patients without dream enactment behavior. Clin Neurol Neurosurg 2006;108:129-34.
29. Dugger BN, Murray ME, Boeve BF, Parisi JE, Benarroch EE, Ferman TJ, Dickson DW. Neuropathological analysis of brainstem cholinergic and catecholaminergic nuclei in relation to rapid eye movement (REM) sleep behaviour disorder. Neuropathol Appl Neurobiol 2012;38:142-52.
30. Joza S, Hu MT, Jung KY, Kunz D, Stefani A, Dušek P, et al. Progression of clinical markers in prodromal Parkinson's disease and dementia with Lewy bodies: a multicentre study. Brain 2023;146:3258-72.
31. Zhu RL, Xie CJ, Hu PP, Wang K. Clinical variations in Parkinson's disease patients with or without REM sleep behaviour disorder: a meta-analysis. Sci Rep 2017;7:40779.
32. Xie D, Shen Q, Zhou J, Xu Y. Non-motor symptoms are associated with REM sleep behavior disorder in Parkinson's disease: a systematic review and meta-analysis. Neurol Sci 2021;42:47-60.
33. Valli M, Uribe C, Mihaescu A, Strafella AP. Neuroimaging of rapid eye movement sleep behavior disorder and its relation to Parkinson's disease. J Neurosci Res 2022;100:1815-33.
34. Donzuso G, Cicero CE, Giuliano L, Squillaci R, Luca A, Palmucci S, Basile A, Lanza G, Ferri R, Zappia M, Nicoletti A. Neuroanatomical findings in isolated REM sleep behavior disorder and early Parkinson's disease: a Voxel-based morphometry study. Brain Imaging Behav 2024;18:83-91.
35. Campabadal A, Abos A, Segura B, Serradell M, Uribe C, Baggio HC, Gaig C, Santamaria J, Compta Y, Bargallo N, Junque C, Iranzo A. Disruption of posterior brain

functional connectivity and its relation to cognitive impairment in idiopathic REM sleep behavior disorder. Neuroimage Clin 2020;25:102138.
36. Yoon EJ, Lee JY, Nam H, Kim HJ, Jeon B, Jeong JM, Kim YK. A New Metabolic Network Correlated with Olfactory and Executive Dysfunctions in Idiopathic Rapid Eye Movement Sleep Behavior Disorder. J Clin Neurol 2019;15:175-83.
37. Liu J, Shuai G, Fang W, Zhu Y, Chen H, Wang Y, Li Q, Han Y, Zou D, Cheng O. Altered regional homogeneity and connectivity in cerebellum and visual-motor relevant cortex in Parkinson's disease with rapid eye movement sleep behavior disorder. Sleep Med 2021;82:125-33.
38. Jiang X, Wu Z, Zhong M, Shen B, Zhu J, Pan Y, Yan J, Zhang W, Xu P, Xiao C, Zhang L. Abnormal Gray Matter Volume and Functional Connectivity in Parkinson's Disease with Rapid Eye Movement Sleep Behavior Disorder. Parkinsons Dis 2021;2021:8851027.
39. Lanza G, Aricò D, Lanuzza B, Cosentino FII, Tripodi M, Giardina F, Bella R, Puligheddu M, Pennisi G, Ferri R, Pennisi M. Facilitatory/inhibitory intracortical imbalance in REM sleep behavior disorder: early electrophysiological marker of neurodegeneration? Sleep 2020;43:zsz242.
40. Borghammer P. The α-Synuclein Origin and Connectome Model (SOC Model) of Parkinson's Disease: Explaining Motor Asymmetry, Non-Motor Phenotypes, and Cognitive Decline. J Parkinsons Dis 2021;11:455-74.
41. Buckner RL, Sepulcre J, Talukdar T, Krienen FM, Liu H, Hedden T, Andrews-Hanna JR, Sperling RA, Johnson KA. Cortical hubs revealed by intrinsic functional connectivity: mapping, assessment of stability, and relation to Alzheimer's disease. J Neurosci 2009;29:1860-73.
42. Zuo XN, Ehmke R, Mennes M, Imperati D, Castellanos FX, Sporns O, Milham MP. Network centrality in the human functional connectome. Cereb Cortex 2012;22:1862-75.
43. Guo M, Ren Y, Yu H, Yang H, Cao C, Li Y, Fan G. Alterations in Degree Centrality and Functional Connectivity in Parkinson's Disease Patients With Freezing of Gait: A Resting-State Functional Magnetic Resonance Imaging Study. Front Neurosci 2020;14:582079.
44. Shan A, Zhang H, Gao M, Wang L, Cao X, Gan C, Sun H, Yuan Y, Zhang K. Aberrant voxel-based degree centrality and functional connectivity in Parkinson's disease patients with fatigue. CNS Neurosci Ther 2023;29:2680-9.
45. Wang H, Chen H, Wu J, Tao L, Pang Y, Gu M, Lv F, Luo T, Cheng O, Sheng K, Luo J, Hu Y, Fang W. Altered resting-state voxel-level whole-brain functional connectivity in depressed Parkinson's disease. Parkinsonism Relat Disord 2018;50:74-80.
46. Seth AK, Barrett AB, Barnett L. Granger causality analysis in neuroscience and neuroimaging. J Neurosci 2015;35:3293-7.
47. Postuma RB, Berg D, Stern M, Poewe W, Olanow CW, Oertel W, Obeso J, Marek K, Litvan I, Lang AE, Halliday G, Goetz CG, Gasser T, Dubois B, Chan P, Bloem BR, Adler CH, Deuschl G. MDS clinical diagnostic criteria for Parkinson's disease. Mov Disord 2015;30:1591-601.
48. Nomura T, Inoue Y, Kagimura T, Uemura Y, Nakashima K. Utility of the REM sleep behavior disorder screening questionnaire (RBDSQ) in Parkinson's disease patients. Sleep Med 2011;12:711-3.
49. Banwinkler M, Dzialas V; Hoenig MC, van Eimeren T. Gray Matter Volume Loss in Proposed Brain-First and Body-First Parkinson's Disease Subtypes. Mov Disord 2022;37:2066-74.
50. Chahine LM, Daley J, Horn S, Colcher A, Hurtig H, Cantor C, Dahodwala N. Questionnaire-based diagnosis of REM sleep behavior disorder in Parkinson's disease. Mov Disord 2013;28:1146-9.
51. Stiasny-Kolster K, Mayer G, Schäfer S, Möller JC, Heinzel-Gutenbrunner M, Oertel WH. The REM sleep behavior disorder screening questionnaire--a new diagnostic instrument. Mov Disord 2007;22:2386-93.
52. Stiasny-Kolster K, Sixel-Döring F, Trenkwalder C, Heinzel-Gutenbrunner M, Seppi K, Poewe W, Högl B, Frauscher B. Diagnostic value of the REM sleep behavior disorder screening questionnaire in Parkinson's disease. Sleep Med 2015;16:186-9.
53. Tomlinson CL, Stowe R, Patel S, Rick C, Gray R, Clarke CE. Systematic review of levodopa dose equivalency reporting in Parkinson's disease. Mov Disord 2010;25:2649-53.
54. Högl B, Arnulf I, Comella C, Ferreira J, Iranzo A, Tilley B, Trenkwalder C, Poewe W, Rascol O, Sampaio C, Stebbins GT, Schrag A, Goetz CG. Scales to assess sleep impairment in Parkinson's disease: critique and recommendations. Mov Disord 2010;25:2704-16.
55. Li S, Ma X, Huang R, Li M, Tian J, Wen H, Lin C, Wang T, Zhan W, Fang J, Jiang G. Abnormal degree centrality in neurologically asymptomatic patients with end-stage renal disease: A resting-state fMRI study. Clin Neurophysiol 2016;127:602-9.
56. Poldrack RA, Huckins G, Varoquaux G. Establishment of Best Practices for Evidence for Prediction: A Review.

JAMA Psychiatry 2020;77:534-40.
57. Tessitore A, Esposito F, Monsurrò MR, Graziano S, Panza D, Russo A, Migliaccio R, Conforti FL, Morrone R, Quattrone A, Di Salle F, Tedeschi G. Subcortical motor plasticity in patients with sporadic ALS: An fMRI study. Brain Res Bull 2006;69:489-94.
58. Mazza S, Soucy JP, Gravel P, Michaud M, Postuma R, Massicotte-Marquez J, Decary A, Montplaisir J. Assessing whole brain perfusion changes in patients with REM sleep behavior disorder. Neurology 2006;67:1618-22.
59. Li D, Huang P, Zang Y, Lou Y, Cen Z, Gu Q, Xuan M, Xie F, Ouyang Z, Wang B, Zhang M, Luo W. Abnormal baseline brain activity in Parkinson's disease with and without REM sleep behavior disorder: A resting-state functional MRI study. J Magn Reson Imaging 2017;46:697-703.
60. Rahayel S, Postuma RB, Montplaisir J, Bedetti C, Brambati S, Carrier J, Monchi O, Bourgouin PA, Gaubert M, Gagnon JF. Abnormal Gray Matter Shape, Thickness, and Volume in the Motor Cortico-Subcortical Loop in Idiopathic Rapid Eye Movement Sleep Behavior Disorder: Association with Clinical and Motor Features. Cereb Cortex 2018;28:658-71.
61. Wakasugi N, Togo H, Mukai Y, Nishikawa N, Sakamoto T, Murata M, Takahashi Y, Matsuda H, Hanakawa T. Prefrontal network dysfunctions in rapid eye movement sleep behavior disorder. Parkinsonism Relat Disord 2021;85:72-7.
62. Arnulf I. REM sleep behavior disorder: motor manifestations and pathophysiology. Mov Disord 2012;27:677-89.
63. De Cock VC, Vidailhet M, Leu S, Texeira A, Apartis E, Elbaz A, Roze E, Willer JC, Derenne JP, Agid Y, Arnulf I. Restoration of normal motor control in Parkinson's disease during REM sleep. Brain 2007;130:450-6.
64. Zang ZX, Yan CG, Dong ZY, Huang J, Zang YF. Granger causality analysis implementation on MATLAB: a graphic user interface toolkit for fMRI data processing. J Neurosci Methods 2012;203:418-26.
65. Zhou Z, Wang X, Klahr NJ, Liu W, Arias D, Liu H, von Deneen KM, Wen Y, Lu Z, Xu D, Liu Y. A conditional Granger causality model approach for group analysis in functional magnetic resonance imaging. Magn Reson Imaging 2011;29:418-33.
66. Sacheli MA, Neva JL, Lakhani B, Murray DK, Vafai N, Shahinfard E, English C, McCormick S, Dinelle K, Neilson N, McKenzie J, Schulzer M, McKenzie DC, Appel-Cresswell S, McKeown MJ, Boyd LA, Sossi V, Stoessl AJ. Exercise increases caudate dopamine release and ventral striatal activation in Parkinson's disease. Mov Disord 2019;34:1891-900.
67. Kaplan A, Mizrahi-Kliger AD, Israel Z, Adler A, Bergman H. Dissociable roles of ventral pallidum neurons in the basal ganglia reinforcement learning network. Nat Neurosci 2020;23:556-64.
68. Rodriguez-Porcel F, Wilmskoetter J, Cooper C, Taylor JA, Fridriksson J, Hickok G, Bonilha L. The relationship between dorsal stream connections to the caudate and verbal fluency in Parkinson disease. Brain Imaging Behav 2021;15:2121-5.
69. Villablanca JR. Counterpointing the functional role of the forebrain and of the brainstem in the control of the sleep-waking system. J Sleep Res 2004;13:179-208.
70. Zhang X, Chai C, Ghassaban K, Ye J, Huang Y, Zhang T, Wu W, Zhu J, Zhang X, Haacke EM, Wang Z, Xue R, Xia S. Assessing brain iron and volume of subcortical nuclei in idiopathic rapid eye movement sleep behavior disorder. Sleep 2021;44:zsab131.
71. Kim YE, Kim YJ, Hwang HS, Ma HI. REM sleep behavior disorder in early Parkinson's disease predicts the rapid dopaminergic denervation. Parkinsonism Relat Disord 2020;80:120-6.
72. Yoon EJ, Monchi O. Probable REM sleep behavior disorder is associated with longitudinal cortical thinning in Parkinson's disease. NPJ Parkinsons Dis 2021;7:19.
73. Figorilli M, Lanza G, Congiu P, Lecca R, Casaglia E, Mogavero MP, Puligheddu M, Ferri R. Neurophysiological Aspects of REM Sleep Behavior Disorder (RBD): A Narrative Review. Brain Sci 2021;11:1588.
74. Lanza G, Fisicaro F, Cantone M, Pennisi M, Cosentino FII, Lanuzza B, Tripodi M, Bella R, Paulus W, Ferri R. Repetitive transcranial magnetic stimulation in primary sleep disorders. Sleep Med Rev 2023;67:101735.
75. Anderson RJ, Aldridge JW, Murphy JT. Function of caudate neurons during limb movements in awake primates. Brain Res 1979;173:489-501.
76. Han XH, Li XM, Tang WJ, Yu H, Wu P, Ge JJ, Wang J, Zuo CT, Shi KY. Assessing gray matter volume in patients with idiopathic rapid eye movement sleep behavior disorder. Neural Regen Res 2019;14:868-75.
77. Campabadal A, Segura B, Junque C, Serradell M, Abos A, Uribe C, Baggio HC, Gaig C, Santamaria J, Compta Y, Bargallo N, Iranzo A. Cortical Gray Matter and Hippocampal Atrophy in Idiopathic Rapid Eye Movement Sleep Behavior Disorder. Front Neurol 2019;10:312.
78. Radziunas A, Deltuva VP, Tamasauskas A, Gleizniene R,

Pranckeviciene A, Petrikonis K, Bunevicius A. Brain MRI morphometric analysis in Parkinson's disease patients with sleep disturbances. BMC Neurol 2018;18:88.
79. Borek LL, Kohn R, Friedman JH. Phenomenology of dreams in Parkinson's disease. Mov Disord 2007;22:198-202.
80. Poryazova R, Oberholzer M, Baumann CR, Bassetti CL. REM sleep behavior disorder in Parkinson's disease: a questionnaire-based survey. J Clin Sleep Med 2013;9:55-9A.
81. Ohlhauser L, Smart CM, Gawryluk JR. Tract-Based Spatial Statistics Reveal Lower White Matter Integrity Specific to Idiopathic Rapid Eye Movement Sleep Behavior Disorder as a Proxy for Prodromal Parkinson's Disease. J Parkinsons Dis 2019;9:723-31.
82. Sun J, Ma J, Gao L, Wang J, Zhang D, Chen L, Fang J, Feng T, Wu T. Disruption of locus coeruleus-related functional networks in Parkinson's disease. NPJ Parkinsons Dis 2023;9:81.
83. Riederer P, Jellinger KA, Kolber P, Hipp G, Sian-Hülsmann J, Krüger R. Lateralisation in Parkinson disease. Cell Tissue Res 2018;373:297-312.

Cite this article as: Shan AD, Zhang H, Gao MX, Wang LN, Cao XY, Gan CT, Sun HM, Lu QL, Zhang L, Yuan YS, Zhang KZ. Altered effective connectivity in Parkinson's disease patients with rapid eye movement sleep behavior disorder: a resting-state functional magnetic resonance imaging study and support vector machine analysis. Quant Imaging Med Surg 2025;15(1):352-369. doi: 10.21037/qims-24-1196

